# Acoustics, Stability, and Compensation in Boiling Water Reactor Pressure Control Systems

HARRY G. KWATNY, MEMBER, IEEE, AND LESTER H. FINK, FELLOW, IEEE

*Abstract*—**An analysis is provided of the effects of steam pipe acoustics on the control of steam pressure in boiling water reactors. A model is developed for the process which encompasses the reactor vessel, the main steam piping, the bypass system piping, the turbine throttle valve and bypass valve, and associated control equipment. It is shown that instability of the closed loop can occur unless the acoustics are suitably accounted for. Moreover, it is shown that although classical compensation schemes may lead to adequate controller designs in some situations, such regulators are limited in their ability to provide fast pressure recovery and can thus contribute to undesirable oscillations between reactor pressure and water level control loops. State variable methods are shown to lead to fundamentally different control structures which eliminate this difficulty but other considerations are noted which can limit their application. These are, however, minor when compared to the benefits attainable.**

## INTRODUCTION

THE CONTROL of steam pressure in boiling water reactor (BWR) nuclear power stations is one of the critical plant automatic control functions. In typical units, during normal load following, pressure is regulated by manipulation of the turbine admission valves [1]. Power output is controlled over a limited range (about 25–35 percent) by adjustment of the reactor recirculation flow. Control rod adjustments are made when larger power changes are required. An increased generation requirement would cause the recirculation flow to increase resulting in an increased steaming rate. The turbine admission valves would then open in response to the consequent increase in reactor pressure. For faster response a feedforward signal is frequently used to temporarily adjust (lower, in the case of a load increase) the pressure regulator set point.

Pressure is regulated by the use of turbine bypass valves during start-up as well as during and following rapid closure of the turbine admission valves. The latter would take place in a variety of abnormal situations calling for full or partial load rejection. The bypass valves admit steam directly into the condenser as illustrated in Fig. 1.

A major control loop which can significantly interact with pressure regulation is the feedwater control loop which adjusts feedwater flow in order to maintain reactor water level within prescribed limits. Incoming feedwater is directed into the recirculation flow stream thus causing the water entering the core to be subcooled. The degree of subcooling affects the core energy balance in a fairly complex manner thus affecting reactor steaming rate and ultimately pressure. Lightly damped oscillations between the pressure and feedwater control loops can be troublesome particularly at low power levels.

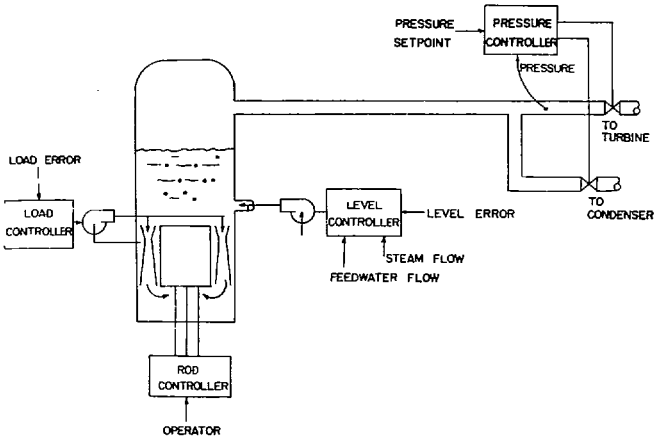


Fig. 1. Schematic of representative boiling water reactor power plant.

The principal mechanisms through which the dynamics of these control loops interact are associated with core reactivity phenomena [2], [3]. Roughly speaking, the time rate of change of power level is proportional to the product of power level and the core power coefficient of reactivity. Reactivity can be affected by a number of factors, the most significant from a control point of view being control rod position and coolant void fraction. The reactivity coefficient represents the fractional net excess neutron production over that necessary to maintain the existing neutron density or power level. At equilibrium the coefficient of reactivity is zero. A positive coefficient indicates that, on the average, each neutron produced during the fission process in turn produces more than one fission destined neutron, hence causing the neutron density, and consequently power, to increase. Insertion of control rods removes neutrons by absorption thus lowering the coefficient.

Since the energy range where the highest probability of fission exists is lower than that of newly produced neutrons, the coefficient of reactivity will be increased by moderating (slowing down) the high energy neutrons. A decrease in core steam voids increases the fluid density in the core thus improving the fluid moderating efficiency and consequently giving rise to an increasing power level. The void fraction of the coolant depends upon the heat

Manuscript received November 7, 1974; revised July 7, 1975. Paper recommended by B. Friedland, Chairman of the IEEE S-CS Applications, Systems Evaluation, Components Committee.

H. G. Kwatny is with the College of Engineering, Drexel University, Philadelphia, Pa.

L. H. Fink is with the U.S. Energy Research and Development Administration, Rockville, Md.

transferred from the fuel, the coolant flow rate (recirculation rate), the coolant core inlet temperature (or, equivalently, subcooling) and the reactor pressure. Heat flux depends principally on power level and gives rise to a relatively high-gain negative feedback of power level through the void fraction mechanism. This is referred to as the void reactivity feedback loop.

Increasing the recirculation rate or the subcooling results in a decreased coolant void fraction and consequently increased power level. Recirculation rate is a primary means for regulating power level in modern BWR direct cycle power plants as described above. Pressure effects on power level through the void fraction mechanism are of three types: direct compression or expansion of steam voids; change of the saturation enthalpy and therefore the subcooling; condensation of saturated steam or flashing of saturated water. The last is by far the most significant. At rated Dresden conditions, for example, a sudden 20 lb/in$^2$ increase in pressure would cause about a 10 percent decrease in core void fraction [2].

As a result of this sensitivity, high quality pressure regulation is an essential ingredient of all aspects of BWR power plant operation. Fortunately, because of its importance in all forms of steam power production, the technology of pressure control in such applications has developed to a fairly sophisticated state. Heretofore, the essential process dynamics of concern have been associated with the valve actuator and pressure vessel mass storage. Although a simple process on the surface, a number of subtleties do arise as described in [4]. In modern, large scale BWR applications a new complication has been recognized. Because of the necessary long length of steam leads from the reactor vessel to the turbine admission valves and bypass valves the piping dynamics can become significant. Field experience has indicated that otherwise desirable high-loop gains can cause sustained oscillations at frequencies near the acoustic resonant frequencies of the main steam piping.

In this paper a model is developed for the analysis of such pressure control systems and which includes a representation of steam pipe acoustic phenomena. It is shown how pipe dynamics interact with other relevent process dynamics and how, under certain conditions, instabilities can be introduced by attempts to tightly regulate reactor pressure without suitable compensation for acoustic behavior. Current procedures for dealing with this problem are reviewed and the limitations of these solutions are noted.

The application of state variable techniques to compensator design for this process is shown to lead to a class of compensators fundamentally different from those developed from classical considerations. It is observed that in certain situations there is the potential for very substantial performance improvement; however, there is also the danger of limit cycling in the presence of excessive deadbands.

## Model Development

In this section a model is developed for use in the analysis of BWR pressure control systems. The overall configuration is illustrated in Fig. 2.

For the purposes of presenting a reasonably compact and useful analysis of the essentials of pressure regulation a number of simplifying assumptions are made. These include the following.

1) Pressure is uniform throughout the reactor steam dome and the contents are saturated vapor at the reactor pressure.

2) Reactor evaporation rate is constant.

3) Steam dome volume is constant.

4) There is negligible energy loss in piping either through heat transfer or friction.

5) A linear model is desired and suitable.

The development proceeds by first considering an individual pipe section, then the overall pipe configuration (consisting of three pipe sections), and finally adding the reactor and valve equations. After completing the general model, advantage is taken of the existence of a natural division of time constants so that a simplified model is obtained which can be subjected to detailed analysis.

### *Pipe Section*

Consider a section of pipe of length $L$ and let $x$ ($0 \leqslant x \leqslant L$) denote displacement along the length of the pipe. Each fluid particle is identified by its position $x = X$ at time $t_0$. The displacement function $x = \bar{x}(X,t)$ denotes the location of a fluid particle at time $t$ which occupied the position $x = X$ at time $t_0$. Similarly, the density and pressure of that particle are represented by the functions $\rho(X,t)$, $p(X,t)$. The relative displacement function is defined as $\xi(X,t) = \bar{x}(X,t) - X$, and the relative velocity function is $v(X,t) = \partial \xi(X,t)/\partial t$.

For the purposes of providing a reasonably simplified analysis, the following assumptions are made.

1) The flow is isentropic.

2) Density variations are small (acoustic approximation)

$$\rho(X,t) - \rho^* = \rho^* \phi(X,t), \qquad \phi(X,t) \ll 1. \tag{1}$$

In this case, the relevent physical equations are [5]:

conservation of mass
$$\frac{\partial \xi}{\partial X} = -\phi \tag{2}$$

conservation of momentum
$$\frac{\partial^2 \xi}{\partial t^2} = -c^2 \frac{\partial \phi}{\partial X} \tag{3}$$

constitutive relation
$$p(X,t) - p^* = \rho^* c^2 \phi(X,t) \tag{4}$$

where $c$ is the velocity of sound, defined by

$$c^2 = \left( \frac{\partial p}{\partial \rho} \right)_s. \tag{5}$$

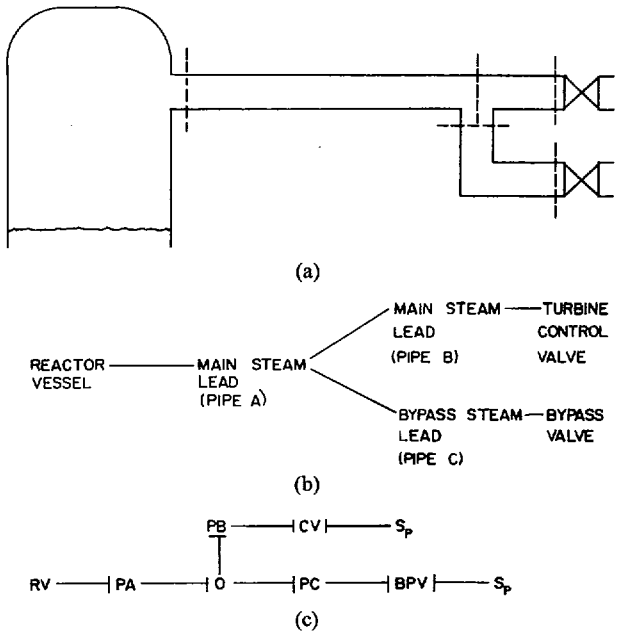


Fig. 2. Model schematic and bond graph. (a) Schematic of process. (b) Word bond graph. (c) Bond graph.

Equations (2) and (3) can be combined to yield

$$\frac{1}{c^2}\frac{\partial^2 \xi}{\partial t^2} = \frac{\partial^2 \xi}{\partial X^2}, \qquad 0 \leqslant X \leqslant L \tag{6}$$

which is subject to the following boundary conditions.

1) Pressure is specified at the inlet, or equivalantly $\phi$ is specified according to

$$\phi_0(t) = (p(0,t) - p^*)/\rho^* c^2 \tag{7}$$

so that

$$\frac{\partial \xi}{\partial X} = -\phi_0 \quad \text{at} \quad X = 0. \tag{8}$$

2) Relative velocity is specified at the outlet boundary so that

$$\frac{\partial \xi}{\partial t} = v_1(t) \quad \text{at} \quad X = L. \tag{9}$$

Taking the Laplace transform of the time variable, the velocity and acoustic parameter distributions are readily obtained

$$V(X,s) = \left\{ \frac{e^{-\frac{s}{c}X} + e^{\frac{s}{c}X}}{e^{-\frac{s}{c}L} + e^{\frac{s}{c}L}} \right\} V(L,s) + \left\{ \frac{-e^{-\frac{s}{c}(L-x)} + e^{\frac{s}{c}(L-x)}}{e^{-\frac{s}{c}L} + e^{\frac{s}{c}L}} c \right\} \Phi(0,s)$$

$$\Phi(X,s) = \left\{ \frac{e^{-\frac{s}{c}X} - e^{\frac{s}{c}X}}{e^{-\frac{s}{c}L} + e^{\frac{s}{c}L}} \right\} \frac{V(L,s)}{c} + \left\{ \frac{e^{-\frac{s}{c}(L-X)} + e^{\frac{s}{c}(L-X)}}{e^{-\frac{s}{c}L} + e^{\frac{s}{c}L}} \right\} \Phi(0,s). \tag{10}$$

*Pipe Configuration*

The velocity and acoustic parameter distributions throughout the piping arrangement illustrated in Fig. 2 can be determined. Note that the boundary conditions are the acoustic parameter (pressure) at the inlet to pipe $A$ and the fluid velocities at the outlets of pipes $B$ and $C$.

Let

$$G_i(X_i,s) = \frac{e^{-\frac{s}{c}X_i} + e^{\frac{s}{c}X_i}}{e^{-\frac{s}{c}L_i} + e^{\frac{s}{c}L_i}}, \qquad i = A,B,C$$
$$F_i(X_i,s) = \frac{e^{-\frac{s}{c}(L_i - X_i)} + e^{\frac{s}{c}(L_i - X_i)}}{e^{-\frac{s}{c}L_i} + e^{\frac{s}{c}L_i}}. \tag{11}$$

Then

$$V_i(X_i,s) = G_i(X_i,s)V_i(L_i,s) + F_i(X_i,s)\Phi_i(0,s), \qquad i = A,B,C. \tag{12}$$

At the pipe junction, the appropriate boundary conditions are

$$\Phi_A(L_A,s) = \Phi_B(0,s) = \Phi_C(0,s)$$
$$A_A V_A(L_A,s) = A_B V_B(0,s) + A_C V_C(0,s) \tag{13}$$

which, respectively, represent equal pressure at the junction and continuity of mass.

The relations

$$\Phi_i(X_i,s) = -\frac{1}{s}\frac{\partial V_i(X_i,s)}{\partial X_i}, \qquad i = A,B,C \tag{14}$$

are obtained from (2) by differentiation with respect to $t$. Denoting

$$G_i'(X_i,s) = \frac{\partial G_i(X_i,s)}{\partial X_i}, \qquad F_i'(X_i,s) = \frac{\partial F_i(X_i,s)}{\partial X_i} \tag{15}$$

(12) can be resolved to yield the acoustic parameter at the junction

$$\Phi_A(L_A,s) = \{s + G_A'(L_A,s)[\alpha F_B(0,s) + \beta F_C(0,s)]\}^{-1} \cdot \{-G_A'(L_A,s)[\alpha G_B(0,s)V_B(L_B,s) + \beta G_C(0,s)V_C(L_C,s)] - F_A'(L_A,s)\Phi_A(0,s)\} \tag{16}$$

where

$$\alpha = A_B/A_A, \qquad \beta = A_C/A_A.$$

The velocity distributions are then given by

$$V_A(X_A,s) = G_A(X_A,s)\{\alpha V_B(0,s) + \beta V_C(0,s)\} + F_A(X_A,s)\Phi_A(0,s)$$

$$V_i(X_i,s)=G_i(X_i,s)V_i(L_i,s)+F_i(x_i,s)\Phi_A(L_A,s), \quad i=B,C \quad (17)$$

and acoustic parameter distributions can now be obtained using (14).

In the special case where $L_B \ll L_A$, $L_C$, which is the common situation, the pipe junction acoustic parameter $\Phi_A(L_A,s)$ characterizes the turbine throttle valve pressure and the measured (controlled) pressure. With $L_B=0$ the following are obtained:

$$G_B(0,s)=1, \quad F_B(0,s)=0$$

which lead to the equations

$$\Phi_A(L_A,s)=\{s+\beta G_A'(L_A,s)F_C(0,s)\}^{-1}\{-G_A'(L_A,s)\cdot[\alpha V_B(L_B,s)+\beta G_C(0,s)V_C(L_C,s)]-F_A'(L_A,s)\Phi_A(0,s)\} \quad (18)$$

$$V_A(X_A,s)=G_A(X_A,s)\{\alpha V_B(0,s)+\beta V_C(0,s)\}+F_A(x_A,s)\Phi_A(0,s)$$

$$V_B(0,s)=V_B(L_B,s) \quad (19)$$

$$V_C(X_C,s)=G_C(X_C,s)V_C(L_C,s)+F_C(X_C,s)\Phi_A(L_a,s)$$

$$\Phi_A(X_A,s)=-\frac{1}{s}G_A'(X_A,s)\{\alpha V_B(0,s)+\beta V_C(0,s)\}-\frac{1}{s}F_A'(X_A,s)\Phi_A(0,s) \quad (20)$$

$$\Phi_C(X_C,s)=-\frac{1}{s}G_C'(X_C,s)V_C(L_C,s)-F_C'(X_C,s)\Phi_A(L_A,s).$$

These equations allow computation of the velocity and acoustic parameter distributions throughout the system if the inlet acoustic parameter and exit velocity are given as functions of time.

All that is actually required as outputs for interfacing with other system elements and for further analysis, however, are the inlet velocity and exit acoustic parameters. Thus, a suitable description of the system is given by (18) above along with

$$V_A(0,s)=\alpha G_A(0,s)V_B(L_B,s)+\beta G_A(0,s)G_C(0,s)V_C(L_C,s)+F_A(0,s)\Phi_A(0,s)+\beta G_A(0,s)F_C(0,s)\Phi_A(L_A,s) \quad (21)$$

$$\Phi_C(L_C,s)=-\frac{1}{s}G_C'(L_C,s)V_C(L_C,s)-\frac{1}{s}F_C'(L_C,s)\Phi_A(L_A,s). \quad (22)$$

For illustrative purposes, further specialization to the case where $\alpha=\beta=1$ (equal pipe cross-sectional areas) is useful. All relevent behavioral characteristics are retained and the formulas are considerably simplified. Defining $L=L_A+L_C$, (18), (21), and (22) become

$$\Phi_A(L_A,s)=-\frac{1}{2c}\frac{(-e^{-\frac{s}{c}L_A}+e^{\frac{s}{c}L_A})(e^{-\frac{s}{c}L_c}+e^{\frac{s}{c}L_c})}{(e^{-\frac{s}{c}L}+e^{\frac{s}{c}L})}V_B(L_B,s)-\frac{1}{c}\frac{(-e^{-\frac{s}{c}L_A}+e^{\frac{s}{2}L_A})}{(e^{-\frac{s}{c}L}+e^{\frac{s}{c}L})}V_C(L_C,s)+\frac{(e^{-\frac{s}{c}L_c}+e^{\frac{s}{c}L_c})}{(e^{-\frac{s}{c}L}+e^{\frac{s}{c}L})}\Phi_A(0,s) \quad (23)$$

$$V_A(0,s)=\frac{(e^{-\frac{s}{c}L_c}+e^{\frac{s}{c}L_c})}{(e^{-\frac{s}{c}L}+e^{\frac{s}{c}L})}V_B(L_B,s)+\frac{2}{(e^{-\frac{s}{c}L}+e^{\frac{s}{c}L})}V_C(L_C,s)+\frac{c(-e^{-\frac{s}{c}L}+e^{\frac{s}{c}L})}{(e^{-\frac{s}{c}L}+e^{\frac{s}{c}L})}\Phi_A(0,s) \quad (24)$$

$$\Phi_C(L_C,s)=-\frac{1}{c}\frac{(-e^{-\frac{s}{c}L_A}+e^{\frac{s}{c}L_A})}{(e^{-\frac{s}{c}L}+e^{\frac{s}{c}L})}V_B(L_B,s)-\frac{1}{c}\frac{(-e^{-\frac{s}{c}L}+e^{\frac{s}{c}L})}{(e^{-\frac{s}{c}L}+e^{\frac{s}{c}L})}V_C(L_C,s)+\frac{2}{(e^{-\frac{s}{c}L}+e^{\frac{s}{c}L})}\Phi_A(0,s). \quad (25)$$

*Steam Valves*

For small perturbations in valve area and upstream pressure, fluctuation of flow through the valve will depend only on these parameters and consequently steam relative velocity variations $v_{B1}(t)$ and $v_{C1}(t)$ can be approximated by

$$v_{i1}(t)=K_{iu}u_i(t)+K_{i\phi}\phi_i(t), \quad i=B,C. \quad (26)$$

*Reactor*

The reactor is modeled by a mass balance applied to the steam space

$$\frac{d}{dt}(\rho_r V)=w-\rho_r A_A \bar{v}_r \quad (27)$$

where $V$ is the steam space volume, $w$ the evaporation rate, and $\bar{v}_r$ the absolute reactor exit velocity. It is assumed that $V$ and $w$ are constant and that steam thermodynamic conditions are uniform throughout the steam space corresponding to saturated vapor at the reactor pressure $P_r(t)$. The constitutive relation to be used is

$$P_r-P^*=\gamma(\rho_r-\rho^*), \quad \text{where} \quad \gamma=\left(\frac{\partial P}{\partial \rho}\right)_{\text{sat vap at } P^*}. \quad (28)$$

Using the definition $\phi_0=(P_r-P^*)/\rho^* c^2$ and linearizing (27) about $P^*$, $\rho^*$, $v_r^*=w/\rho_r^* A_a$ leads to

$$\frac{d}{dt}\phi_0=\left[-\frac{A_A \bar{v}_r^*}{V}\right]\phi_0-\left[\frac{\gamma A_A}{c^2 V}\right]v_r(t),$$
$$v_r(t)=V_A(0,t). \quad (29)$$

The process model can now be organized in the form of a block diagram as shown in Fig. 3. The transer relations $\Pi$, $\Sigma$, and $\Gamma$ can be identified by comparing Fig. 3 with (23)–(25). $G_r$ is the reactor transfer function corresponding to (29).

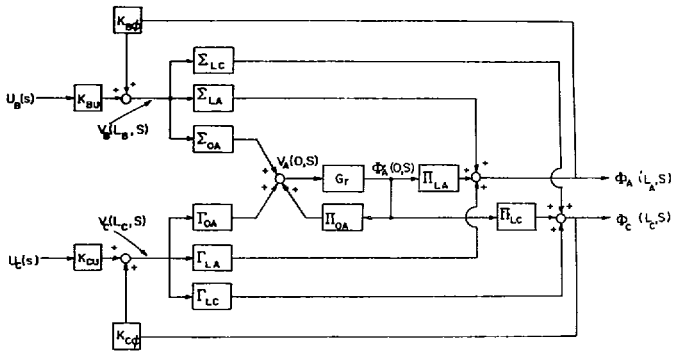

Fig. 3. Process block diagram.

*Simplified Process Model*

A meaningful and far less cumbersome analysis can be conducted in a somewhat restricted scenario. It will be assumed that the main turbine valves are shut so that $v_B(L_B,t)\equiv 0$ and steam flow passes only through the bypass valves. Such a situation would occur during start-up or following a turbine trip.[1] Moreover, the analysis of this situation is not fundamentally different from the case where the bypass valves are closed and all steam passes through the turbine or the case where both sets of valves are open.

In addition, it will be assumed that the reactor time constant is sufficiently large relative to the piping response times that $\Pi_{LA}$, $\Pi_{LC}$ and $\Pi_{0A}$ will be subjected only to (relatively) slowly varying inputs and can thus be approximated by their dc values. Similarly, only the slowly varying outputs of $\Gamma_{0A}$ need be accurately reproduced since high frequency terms will be filtered out by the reactor transfer function. Consequently, the following low frequency approximations are made

$$\Gamma_{0A}\approx 1, \quad \Pi_{LA}\approx 1, \quad \Pi_{LC}\approx 1, \quad \Pi_{0A}\approx 0.$$

The result reduced model is shown in Fig. 4.

*Pole-Zero Locations for Simplified Process Model*

Denoting the plant transfer between the bypass valve area $U_C$ (input) and measured pressure $\Phi_A(L_A,s)$ by $\Gamma(s)$ and using the representation $\Gamma_i(s)=N_i(s)/D_i(s)$ the plant transfer function is found to be

$$\Gamma(s)=\frac{K_{Cu}(N_rD_{LA}+D_rN_{LA})}{(D_r-K_{C\phi}N_r)D_{LC}-K_{C\phi}D_rN_{LC}}. \tag{30}$$

The location of the plant poles depend upon the valve coefficient and satisfy the relation

$$K_{C\phi}\frac{-D_rN_{LC}-N_rD_{LC}}{D_rD_{LC}}=-1. \tag{31}$$

Since $N_r$ is a very small constant, the "open-loop" zeros of (31) are only slightly different from the roots of $D_rN_{LC}=0$

[1]For the analysis to be meaningful following a turbine trip requires sufficient bypass capacity to begin with.

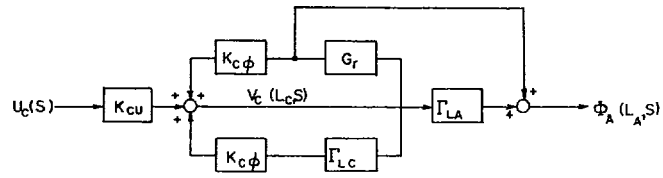

Fig. 4. Block diagram of simplified process model.

and are denoted "modified explain piping zeros" and "modified reactor pole" in Fig. 5. The "open-loop" poles of (31) are the poles of $\Gamma_{LC}$ plus the reactor pole. The location of plant poles as $K_{C\phi}$ varies (positively) is shown in Fig. 5. Note the presence of lightly damped oscillatory modes introduced by the pipe acoustics.

The plant zeros are defined by

$$N_r\frac{D_{LA}}{D_rN_{LA}}=-1. \tag{32}$$

Since $N_r$ is a small constant, the plant zeros can also be approximately located with the aid of a root locus plot as shown in Fig. 6.

## Analysis of the Classical Compensator

Reactor pressure is controlled by regulating the measured throttle pressure $\Phi_A(L_A,s)$ via manipulation of steam flow through bypass valves. The typical feedback control arrangement is illustrated in Fig. 7. Note that dynamics of the valve drive are included. The control problem is to design a compensator which will provide an adequate stability margin and small steady-state pressure errors.

Pressure control systems which vary flow through a valve in order to regulate an upstream pressure have been termed initial pressure control systems by Callan and Eggenberger in a paper [4] in which they present a detailed analysis of several different types of pressure control systems in common use on large steam turbines. The analysis given in [4] assumes a very short steam lead from the primary storage vessel (the reactor in the present case) to the regulating valve. In this case the valve inlet pressure and the vessel pressure are the same, and the principal plant dynamics are simply the storage capacitance of the vessel itself and the valve drive dynamics.

Callan and Eggenberger provide an analysis of proportional, proportional plus reset, and proportional plus partial reset (lag-lead compensation) compensators. They conclude that lag-lead compensation is the most suitable. With the simple proportional system, sufficiently high gain cannot be achieved to satisfy steady-state error requirements without the system becoming unstable. The proportional plus integral controller is rejected because it is unstable for sufficiently low gain (as well as sufficiently high gain) and results in limit cycling in the presence of significant valve drive dead-zone.

Proportional plus integral and lag-lead compensation, with some modification, are in common use today [6], [7]

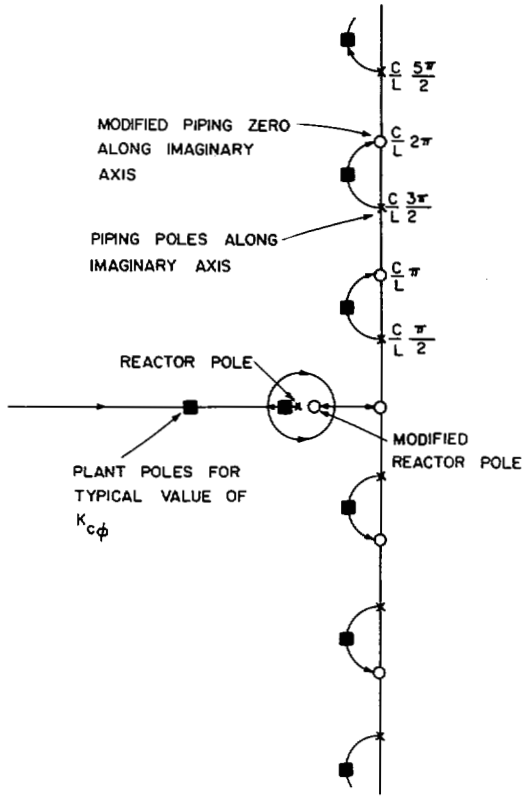


Fig. 5. Location of plant poles (not to scale).

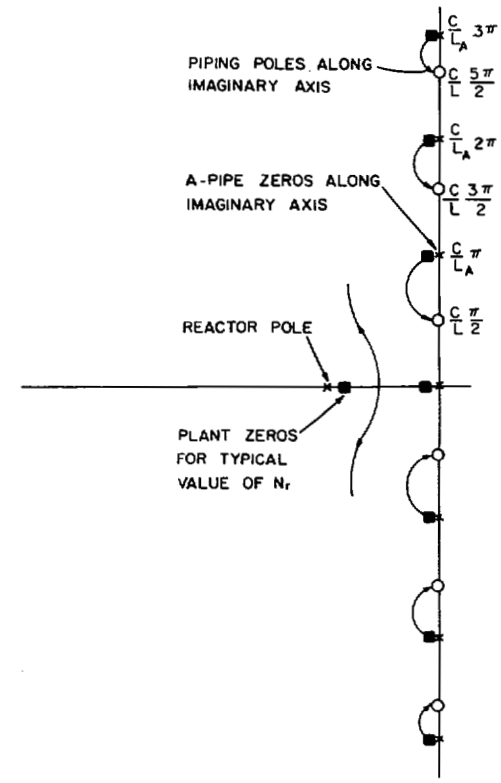


Fig. 6. Location of plant zeros (not to scale).

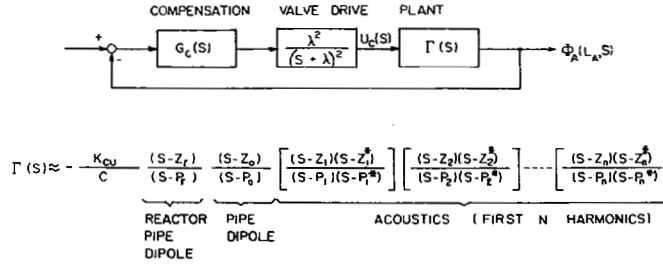


Fig. 7. Block diagram of pressure control system.

even when the steam leads are quite long. Fig. 8 illustrates the application of lag-lead compensation. If sufficient open-loop gain cannot be achieved while maintaining a satisfactory stability margin a band rejection filter can be added, as shown in Fig. 9, to compensate for the first steam line acoustic resonance. In this way the open-loop gain can be increased while maintaining the desired stability margin. For the example system, an improvement of a factor of about three can be achieved.

## Compensation Based on State Variable Methodology

One outstanding fault in the compensation described above is that the closed-loop dynamics becomes dominated by the pair of poles which are associated with the lag compensation and reactor storage volume. This occurs because both the lag pole and reactor pole are trapped near the origin by the zeros introduced by the pipe dynamics. Whether or not this constitutes a problem depends on the source of potential disturbances. A downstream valve closure may not directly excite these modes because of the cancelling effects of the pipe zeros, if the loop gain is sufficiently high. On the other hand, if the loop gain must be limited to avoid introducing acoustic instabilities such cancellation will not take place. In either case disturbances at the reactor end will excite these modes. Pressure variations in the reactor vessel can be initiated by changes in reactor power level or changes in feedwater flow. The quenching effect of increased feedwater flow and the simultaneous sensitivity of flow to reactor pressure particularly at low power levels, in addition to water level shrink-swell phenomena associated with reactor pressure variations results in significant coupling between the reactor water level and pressure control loops.

Poor pressure regulation can have a substantial deleterious effect on water level control and, in fact, could

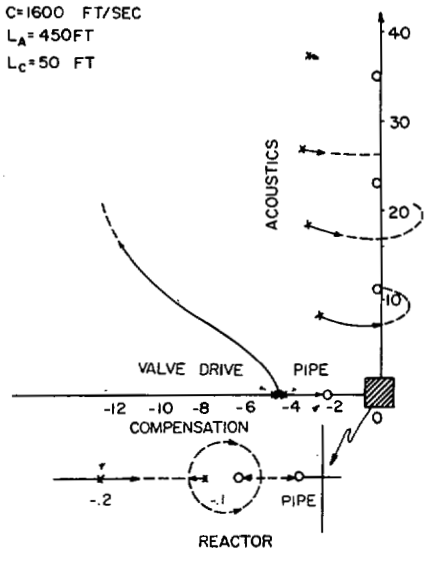


Fig. 8. Root locus with lag-lead compensation.

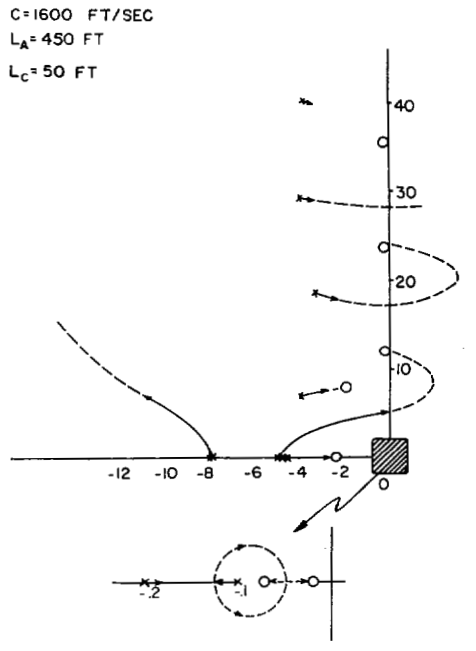


Fig. 9. Root locus with lag-lead and band rejection compensation.

contribute to a high water level trip as a secondary effect following a downstream valve closure (such as during a turbine trip). It is known that increasing the lag time constant too far in order to obtain the consequent advantage in open-loop pressure regulator gain can result in very undesirable lightly damped oscillations between the two control loops.

As a result, there is considerable motivation for further refinement of the compensator in order to increase the speed of the dominant closed-loop modes while maintaining the stability margins and steady-state error coefficients already achieved. Clearly, if further performance improvement is to be attained by additional trial and error modification of the compensator, even more ingenuity will be required than has been applied heretofore. Alternatively, a fresh approach will be attempted in which a compensator is designed from scratch using an approach based on state variable methodology.

*The Design Process*

The general approach to compensator design taken herein is to make use of the concepts of state variable feedback and dynamic observers. A number of specific techniques for doing so have been proposed. The particular procedure used is described in [8], [9] and will only be briefly summarized below. Reset action and higher order control modes are included in this method via the artifice of augmenting the system with random bias variables.

The controller design is based on the model:

$$\begin{aligned} \dot{x} &= Ax + Ew + Bu \\ \dot{w} &= Zw + v \\ y &= Cx + Fw + Du \end{aligned} \tag{33}$$

where $x$ is an $n$-dimensional state vector, $y$ is a $p$-dimensional output vector, $u$ is an $m$-dimensional input vector and $w$ is a $q$-dimensional random bias vector specifically introduced to characterize external disturbances or model inaccuracies. The bias noise $v$ is a white noise process having zero mean and covariance $V_{v\delta}(t)$. The limiting case as $V_v$ vanishes is of particular interest.

The design proceeds in three distinct steps: 1) determination of the nominal (or ultimate state) trajectory, 2) design of the state variable feedback controller, and 3) design of the state and bias variable observer. Each step employs a subset of the output equations as follows. The first step employs the output equations

$$y_1 = C_1 x + F_1 w + D_1 u \tag{34}$$

with $r = \dim(y_1) \leqslant \dim(u)$. Under appropriate conditions the outputs $y_1$ will be driven to desired values $\bar{y}_1$ in ultimate state. In the second step, a (possibly) different set of outputs is employed

$$y_2 = C_2 x + F_2 w + D_2 u. \tag{35}$$

The elements of $y_2$ represent all of those variables which are of concern during the transient. The outputs selected as elements of $y_2$ and the weights given them in the cost functional (if used as described below) shape the character of the transient behavior of the system. The third step, design of the observer-estimator, utilizes a third subset of the output equations

$$y_3 = C_3 x + F_3 w + D_3 u. \tag{36}$$

The outputs included as elements of the $s$-dimensional vector $y_3$ are, of course, only the outputs to be measured. It will be assumed that $C_3$ and $F_3$ are of full rank.

The objective is to steer the system so that $Y_1$ tracks the desired value $\bar{y}_1$ while $u$ varies moderately about the nominal value $\bar{u}$. With $\bar{y}_1$ specified, the appropriate values

of $\bar{x}$, $\bar{u}$ are obtained by setting $v \equiv 0$ in (33) to obtain the ultimate state equations:

$$\begin{aligned} \dot{\bar{x}} &= A\bar{x} + Ew + B\bar{u} \\ \dot{w} &= Zw \\ \bar{y}_1 &= C\bar{x} + Fw + D\bar{u}. \end{aligned} \tag{37}$$

Solutions of the form

$$\begin{aligned} \bar{x} &= X_1\bar{y} + X_2 w \\ \bar{u} &= U_1\bar{y} + U_2 w \end{aligned} \tag{38}$$

are frequently obtainable and are sought by direct substitution in (37).

The state variable feedback gain matrix $K$ can be selected by any of several procedures such as minimization of a quadratic performance index or by pole shifting. The control is then given by

$$u_1 = -M\hat{x}_1, \quad M = \left[ K \mid -KX_2 \; -U_2 \right]$$

where

$$u_1 \triangleq u - U_1\bar{y}_1, \quad x_1 \triangleq \begin{bmatrix} x - X_1\bar{y}_1 \\ w \end{bmatrix} \tag{39}$$

and $\hat{x}_1$ is an estimate of $x_1$ as defined below.

The estimate $\hat{x}_1$ is given by

$$\hat{x}_1 = H^*(y_3 - D_3u_1) + \theta_2\xi \tag{40a}$$

$$\dot{\xi} = (\Lambda A, \theta_2)\xi + (\Lambda B_1)u_1 + (\Lambda A_1 H^*)(y_3 - D_3u_1) \tag{40b}$$

where the parameters are defined below. The following matrices are introduced

$$A_1 = \begin{bmatrix} A & E \\ 0 & Z \end{bmatrix}, \quad H = \underbrace{[H_1}_{n+q-s} \mid \underbrace{H_2]}_{s} = [C_3 \mid F_3],$$

$$G = \begin{bmatrix} 0_{n\times q} \\ \hline I_q \end{bmatrix}, \quad B_1 = \begin{bmatrix} B \\ \hline 0_{q\times m} \end{bmatrix}$$

$$\theta_2 = \begin{bmatrix} I_{n+q-s} \\ \hline -H_2^{-1}H_1 \end{bmatrix},$$

$$H_0^* = \begin{bmatrix} H_{01}^* \\ \hline H_{02}^* \end{bmatrix} \begin{matrix} \updownarrow n+q-s \\ \updownarrow \; s \end{matrix} = (GV_vG')H'(F_3V_2F_3')^{-1}$$

$$\Lambda_0 = \left[ I_{n+q-s} \; -H_{01}^*H_1 \mid -H_{01}^*H_2 \right],$$

$$\mathfrak{M} = \left[ V_2 - V_2F_3'(F_3V_vF_3')^{-1}F_3V_2 \right]. \tag{41}$$

Since $F_3$ is of full rank there is no loss in generality in assuming $H_2$ to be nonsingular. Define $P_{22}$ to be the maximal solution of the Riccati equation:

$$\begin{aligned} &P_{22}(\Lambda_0A_1\theta_2)' + (\Lambda_0A_1\theta_2)P_{22} \\ &- P_{22}(HA_1\theta_2)'(F_3V_2F_3')^{-1}(HA_1\theta_2)P_{22} + \Lambda_0\mathfrak{M}\,\Lambda_0' = 0. \end{aligned} \tag{42}$$

The remaining parameters can now be defined

$$H^* = \begin{bmatrix} H_1^* \\ \hline H_2^* \end{bmatrix} \begin{matrix} \updownarrow n+q-s \\ \updownarrow \; s \end{matrix} = (GV_vG' + P_0A_1')H'(F_3V_2F_3')^{-1}$$

$$P_0 = \theta_2P_{22}\theta_2'$$

$$\Lambda = \left[ I_{n+q-s} \; -H_1^*H_1 \mid -H_2^*H_2 \right]. \tag{43}$$

Alternatively, $H^*$ can be defined as follows. Select a state feedback gain matrix $S$, by any means, which stabilizes the system

$$\dot{z} = (\Lambda_0A_1\theta_2)'z + (HA_1\theta_2)'v, \qquad v = -Sz.$$

Then,

$$H^* = H_0^* + \theta_2S'. \tag{44}$$

The $2n+q$ eigenvalues of the closed-loop system include the $q$ eigenvalues of $Z$ associated with the bias variables $w$, the $n$ stable eigenvalues corresponding to the closed-loop system matrix $\tilde{A} = A - BK$, and the $n+q-s$ eigenvalues of the observer matrix $\Lambda A_1\theta_2$. Moreover, a prescribed degree of stability for the observer is attained by replacing $A_1$ in (42) by $A_1 + \alpha I$, or, in fact, the poles of $\Lambda A_1\theta_2$ can be arbitrarily positioned under general conditions by appropriate selection of $S$.

*The Compensator Formulation*

When (39) and (40) are resolved the equivalent compensator transfer relation is found to be

$$\begin{aligned} U(s) = -\Big\{ &I|sI-\Delta| + \left[ I - MH^*D_3 \right]^{-1} \\ &\cdot M\theta_2\mathrm{Adj}(sI-\Delta)\Omega \Big\}^{-1} \left[ I - MH^*D_3 \right]^{-1} \\ &\cdot M\left\{ I|sI-\Delta| + \theta_2\mathrm{Adj}(sI-\Delta)\Lambda A_1 \right\} H^*Y(s) \end{aligned} \tag{45}$$

where

$$\Delta = \Lambda A_1\theta_2, \quad \Omega = \Lambda B_1 - \Lambda A_1H^*D_3.$$

In the special case where $D_3 = 0$ and $U(s)$, $Y(s)$ are scalars this reduces to

$$\frac{U(s)}{Y(s)} = -MH^* \frac{|sI-\Delta| + M\theta_2\mathrm{Adj}(sI-\Delta)\Lambda A_1H^*/(MH^*)}{|sI-\Delta| + M\theta_2\mathrm{Adj}(sI-\Delta)\Omega}. \tag{46}$$

Now, observe that

$$|A| + a'\mathrm{Adj}(A)b = |A + ba'|$$

for any $n \times n$ matrix $A$ and $n$-dimensional column vectors $a$ and $b$. Consequently, the compensator zeros are defined

by

$$|sI-\Delta|+M\theta_2\mathrm{Adj}(sI-\Delta)\Lambda A_1H'/(MH^*) =|sI-\Lambda A_1[I-H^*M/(MH^*)]\theta_2|=0 \quad (47)$$

and the compensator poles are given by

$$|sI-\Delta|+M\theta_2\mathrm{Adj}(sI-\Delta)\Omega =|sI-\Lambda(A_1-B_1M)\theta_2|=0. \quad (48)$$

*Important Properties of the Compensator*

Consider the special case where $m=q=s$ and $Z=0_{q\times q}$. As shown in [8], the matrix

$$\Gamma_4=\Lambda(A_1-B_1M)\theta_2 \quad (49)$$

will contain $s$ zero eigenvalues. Thus, the compensator includes $s$ zero poles and these, in fact, correspond to reset action and the steady-state error in response to a step change in set point or a step disturbance will be zero.

If $E=0$ and the specified degree of stability of the observer is less than the natural degree of stability of the open-loop system, then $P_0$ will be zero and

$$\Lambda=[I\,|\,0], \quad H^*=\begin{bmatrix}0\\ \hline I\end{bmatrix}. \quad (50)$$

In this case, $\Lambda A_1\theta_2$ reduces to $A$ and $A_1H^*=0$. Consequently, the zeros of the compensator will be the poles of the open-loop system so that the compensator attempts to precisely cancel the dynamics of the system. If a degree of stability is specified greater than the natural degree of stability of the system such cancellation will occur only for those open-loop poles satisfying the stability constraint.

If, in the single input-single output case there is no attempt to alter the natural dynamics of the system, then the state feedback matrix, $K$, is zero and

$$M=[0\,|\,-U_2], \quad (51)$$

and the compensator poles satisfy

$$|sI-\Lambda A_1\theta_2|-U_2C\mathrm{Adj}(sI-\Lambda A_1\theta_2)\Lambda B_1\theta_2=0. \quad (52)$$

With, $E=0$, a stable open-loop system and specification of zero degree of stability this can be written

$$-U_2\frac{C\mathrm{Adj}(sI-A)B}{|sI-A|}=1. \quad (53)$$

Observe that the numerator polynomial is the numerator polynomial of the open-loop system transfer and the denominator is the characteristic polynominal of the open-loop system. Moreover, since $U_2$ is a positive scalar (53) can be thought of as defining the compensator poles via a negative gain root locus. Moreover, as one of the compensator poles is at the origin, one of the root loci must pass through the origin and will define the appropriate value for $U_2$. In addition, for this special case, the compensator zeros cancel the open-loop poles and consequently the closed-loop root locus is defined by [note (48) and (49)]:

$$U_2\frac{C\mathrm{Adj}(sI-A)B}{|sI-\Gamma_4|}=1 \quad (54)$$

and can be interpreted as a positive gain "undoing" of the results of the negative gain process of (53). The proper value of $U_2$ in (54) will result in the closed-loop poles located exactly in the positions of the original open-loop poles.

The special case considered above is of interest for two reasons. First, it provides insight into the mechanisms at work in the design of compensators via the state variable formulation. Second, it provides a solution to a very practical problem: how to design a feedback control system which will precisely steer the system output to any constant desired set-point without causing deterioration of already acceptable, natural dynamics of the process.

*The Pressure Regulator*

It is instructive to consider the case where no attempt is made to alter the natural dynamics of the process. Since, all the conditions prescribed in the previous section are satisfied, the compensator zeros are the process poles and the compensator poles are defined by the negative gain root locus of (53), as illustrated in Fig. 10. The importance of this plot is that it provides an indication of the significance of accounting for the various components of the dynamics of the process. Specifically, the piping dynamics can be approximated by a first, third, fifth, or higher odd order dynamic model by progressively adding representations of higher order acoustic resonance effects. The compensator will attempt to cancel each natural resonant pole with a compensator zero and replace it by a neighboring pole as shown, thus introducing a band rejection filter for each harmonic. As would be expected, the higher the order of the resonance the closer the compensator pole is to the natural pole. The figure clearly suggests that representation of the fourth and higher harmonics is unnecessary and that representation of the first and second is essential.

Of critical importance is the placement of the four compensator poles along the real axis. Essentially, these compensate for the dynamics of the valve drive, reactor storage and the principal mode of the piping. Although the higher order piping dynamics influence the precise positioning of these poles they do not contribute to determination of the general configuration. The pole at the origin is a result of the design requirement of zero steady-state error with respect to constant disturbances. Undoubtedly, the presence of a compensator pole in the right-half plane warrants deeper consideration and will be discussed below.

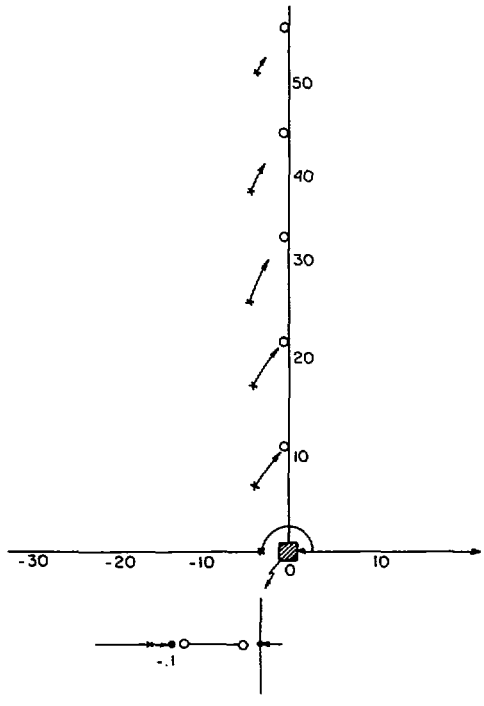


Fig. 10. Root locus for determination of compensator poles.

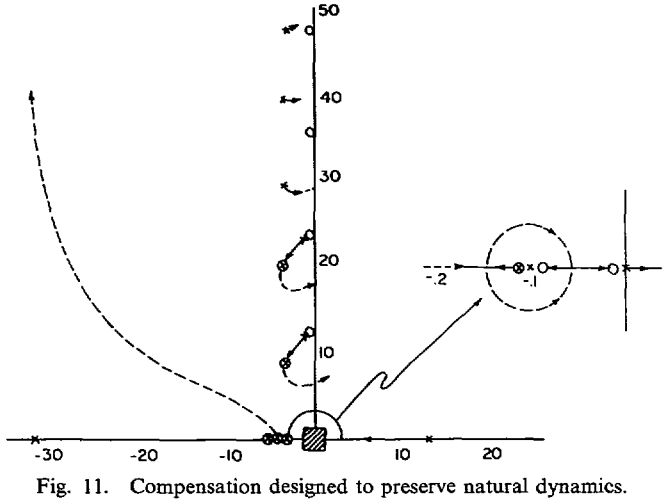


Fig. 11. Compensation designed to preserve natural dynamics.

In the closed-loop, with the ideal gain setting, the poles will be restored to their original position, as shown in Fig. 11. Note that there are now two sets of poles corresponding to the original process poles.[2] These are the closed-loop poles and also the poles cancelled by the compensator and which can be associated with the dynamic observer.

Suppose now that it is desired to constrain the closed-loop system to have time constants no longer than two seconds. This is easily accomplished by selecting a state variable feedback gain matrix which moves the reactor pole only (this is the only violator of the 2 s constraint) to $-0.5$ and by specifiying a degree of stability of 0.5 for the observer. Taking this approach leads to a compensator pole-zero pattern and a closed-loop root locus as shown in Fig. 12. These diagrams illustrate the fact that it is principally the lag-lead dipole introduced by the controller which compensates for the reactor storage volume, at least in the range of speed requirements specified for the example.

### *Some Practical Considerations for Implementation*

The essential novelty of the compensator described above is the presence of a pole in the right-half plane.

[2]This discussion should be interpreted in terms of a finite, although possibly large, dimensional approximate process.

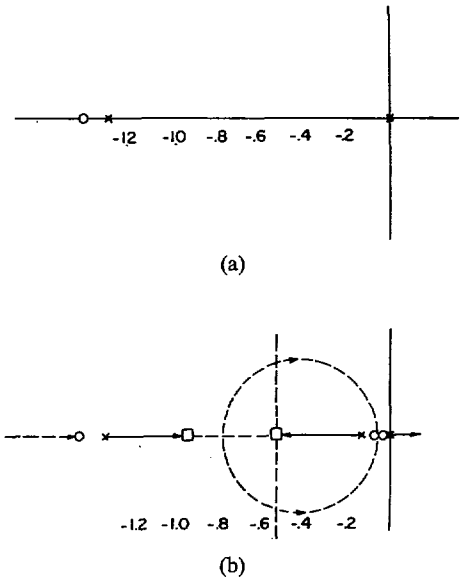


Fig. 12. (a) Compensaror near-origin pole-zero pattern for "sped-up" system. (b) Near-origin root locus for "sped-up" system.

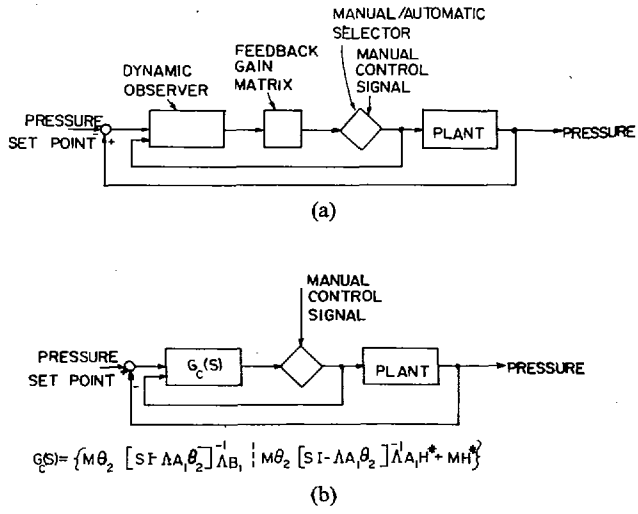


Fig. 13. Implementation of state variable design compensation (feedforward is not shown, $D_3$ assumed zero). (a) General structure. (b) Transfer matrix form.

Through this mechanism complete rejection of constant disturbances can be achieved without forcing a pole to be trapped near the origin by a piping zero. On the other hand, such a device would probably not become a candidate for consideration if the problem were approached classically since the designer would anticipate the need to construct a direct physical realization of the compensator. Although the closed-loop system would be stable, the existence of an unstable element in the open-loop configuration would cause obvious problems.

From the state variable viewpoint, the natural configuration of the controller embodies all of the controller dynamics in a stable observer. The compensator represents only an interpretation of the controller which may be useful for certain types of analysis. Thus, it is the well-behaved observer which needs to be constructed and, consequently, a major contribution of modern state variable control theory is that it expands the class of compensators available for consideration. A reasonable configuration for implementation is illustrated in Fig. 13. Note that with the loop open (manual control) the controller dynamics are those of the stable observer. Since the observer is continuously tracking the plant state and bias variables, a smooth transfer from manual to automatic control can be achieved.

Although the use of an observer, as discussed above, avoids the major obstacle to the application of unstable compensators there are other important considerations. It

has been suggested, by way of example, [10] that unstable compensation can be partner to undesirable sensitivity characteristics. This has not been demonstrated to be generally true. However, unstable compensation does imply that the closed-loop will be unstable for sufficiently low gain. Consequently, the possibility of limit cycling induced by dead bands in the sensor or valve drive becomes a factor of significance. It should be noted that in many existing "classically" compensated systems, dead band induced limit cycles exist and are tolerated so long as they are acceptably small.

## Conclusions

A model has been developed for the analysis of the effects of pipe acoustic phenomena on initial pressure regulators of the type commonly used on BWR nuclear power plants. It has been shown how such pipe dynamics can induce regulator instability for sufficiently high-loop gain. Moreover, it was noted that compensation of the first resonant mode may permit a sizeable increase in loop gain for a given stability margin and can result in satisfactory steady-state and transient performance.

However, it was also observed that a pair of poles are trapped near the origin by pipe zeros when lag-lead compensation is used, with or without compensation for acoustic resonance. The significance of this observation is that interaction between the feedwater control loop and pressure control loop are very undesirable and such a condition is enhanced by the presence of these sluggish modes. With the intent of improving this situation the design of a compensator based on state variable methodology has been considered. It was shown that such a compensator does, indeed, provide the flexibility for improving the closed-loop speed of response while providing zero steady-state error. However, the compensator itself is unstable thus raising questions of its practical suitability.

It has been pointed out that the compensator, in actuality, need not be built, but, alternatively, the appropriate configuration requires construction of a very well-behaved dynamic observer. Moreover, in this configuration, the observer is always active and provides "bumpless" transfer from manual to automatic control. There does remain the problem of limit cycling in the presence of deadband. Application requires that actuator and sensor deadbands be sufficiently small that limit cycle amplitudes will be acceptable. Again, it should be noted that such limit cycling, although undesirable, is frequently tolerated in practice.

Finally, the appearance of a compensator pole in the right half plane is a consequence of the unusual process dynamics which places the dominant zeroes to the right of the dominant poles and the implicit control objectives which are: 1) to place the closed-loop poles in desireable positions, and 2) to maintain a reasonable tolerance on steady-state error. It is not fundamentally a question of state variable versus classical design nor is it a result of the specific requirement of zero steady-state error used herein.

## References


[1] D. G. Carrol, M. A. Eggenberger, and D. N. Ewart, "Response characteristics of boiling water reactor generating units," *IEEE Trans. Power App. Syst.*, vol. PAS-92, pp. 957–960, May/June 1973.

[2] E. R. Owen, "Boiling water reactor control systems," presented at the Nat. Power Conf., Sept. 1962, Paper CPA 62-5108.

[3] S. Glasstone, *Principles of Nuclear Reactor Engineering*. Princeton, N. J.: Van Nostrand, 1961.

[4] P. C. Callan and M. A. Eggenberger, "Basic analysis of pressure-control systems used on large steam turbine-generator units," *Trans. ASME* (J. Eng. Power), pp. 389–400, Oct. 1965.

[5] S. H. Crandall, D. C. Karnapp, E. F. Kurtz, and D. S. Pridmore-Brown, *Dynamics of Mechanical and Electrochemical Systems*. New York: McGraw-Hill, 1968.

[6] D. Nicholson, "Designing and testing for reliability in reactor pressure control systems," *Instrum. Power Ind.*, vol. 14, pp. 62–71, 1971.

[7] L. B. Podolsky, "System and method for operating a boiling water reactor steam power plant," U. S. Patent 3 630 839, Dec. 1971.

[8] H. G. Kwatny, "Optimal linear control theory and a class of PI controllers for process control," in *Proc. 13th Joint Automatic Control Conf.*, Aug. 1972, pp. 274–281.

[9] H. G. Kwatny, J. P. McDonald, and K. C. Kalnitsky, "A class of multivariable controllers and its application to power plant and power system control," in *Proc. 3rd IFAC Symp. Multivariable Technological Systems*, Sept. 1974.

[10] L. Shaw, "Pole placement: Stability and sensitivity of dynamic compensators," *IEEE Trans. Automat. Contr.* (Corresp.), vol. AC-16, p. 210, Apr. 1971.



**Harry G. Kwatny** (M'70) received the B.S. degree in mechanical engineering from Drexel University, Philadelphia, Pa., the S.M. degree in aeronautics and astronautics from the Massachusetts Institute of Technology, Cambridge, and the Ph.D. degree in Electrical Engineering from the University of Pennsylvania, Philadelphia, in 1961, 1962, and 1967, respectively.

During the years 1958–1960 he was involved in testing, modeling, and control development for marine steam generators at the U.S.N. Boiler and Turbine Laboratory, Philadelphia, and from 1962 to 1963 was employed by the U.S.N. Aeronautical Computer Laboratory, Johnsville, Pa., where he was involved in spacecraft simulation and the design of special purpose digital computers. In 1963 he joined Drexel University as an Instructor and is currently Professor of Systems Engineering. Since 1966 he has worked closely with the Research Division of Philadelphia Electric Company in the areas of power plant and power system modeling and control. He is also a consultant to a number of other organizations in the general area of dynamic system analysis. His research and teaching interest include modeling of dynamic systems, control theory and application, stochastic processes, and electric power systems.

Dr. Kwatny is a member of ISA, Pi Tau Sigma, Tau Beta Pi, Phi Kappa Phi, and Sigma Xi.



**Lester H. Fink** (M'51–SM'58'F'73) was born in Philadelphia, Pa., in 1925. He received the B.S. E.E. and the M.S.E.E. degrees from the University of Pennsylvania, in 1950 and 1961, respectively.

From 1950 to 1974, he was employed by the Philadelphia Electric Company, in the Research Division and its predecessor groups. During those years his work involved the application of field theory to underground thermal regimes, the automatic dispatch of electric power, and the modeling, simulation, and control of generating plants and of individual and interconnected power systems. He holds three patents in these areas, and numerous papers by him on these topics have been published in AIEE/IEEE Transactions on Power Apparatus and Systems, *ISA Advances in Instrumentation*, and other periodicals. During these years he

also held the position of Adjunct Professor at Drexel University in both the Department of Electrical Engineering and the Evening College, developing and teaching courses in Automatic Control Theory, Electromagnetic Field Theory, and Electric Power Systems Dynamics. In May 1974 he was employed by the U.S. Department of the Interior, Office of Research and Development, and transferred to the Energy Research and Development Administration at its establishment in January 1975, where, within the Division of Electric Energy Systems, he is Assistant Director for Systems Management and Structuring. His main interests are in the application of systems theory to the structuring and operation of electric energy systems.

Mr. Fink is a Registered Professional Engineer in Pennsylvania, a member of ISA, AAAS, CIGRE, and of Sigma Tau, Eta Kappa Nu, and Tau Beta Pi. He has served as Director of the Automatic Control Systems Division of ISA, and is IEEE representative on the Engineering Foundation Conferences Committee.

# Performance Predictions for High Altitude Self-Contained Satellite Navigation Systems

JOSEPH L. LEMAY, MEMBER, IEEE, WILLIAM L. BROGAN, MEMBER, IEEE, CHARLES E. SEAL, MEMBER, IEEE, AND HOWARD T. HENDRICKSON

*Abstract*—**This paper summarizes a study of self-contained navigation system accuracies for high altitude orbital missions projected through 1985. It is found that root-sum-square (RSS) satellite position errors as low as a few hundred feet are obtainable with range measuring systems. Totally autonomous, nonradiating systems are operationally more attractive, and some promising candidates in this category give RSS position errors from about one-half to a few miles, depending on the orbit. The extended Kalman filter and extensive Monte Carlo simulations are used as the basic analysis tools. Favorable comparisons between covariance analysis and Monte Carlo results are reported. Time-average statistics are also found to provide useful figures of merit.**

## I. Introduction

ASPECTS of the satellite navigation problem have been investigated many times in the past. Gunckel [1] was one of the first, and this work is often cited as the origin of the now routinely used extended Kalman filtering techniques. A sampling of these previous studies may be found in [2]–[8]. Additional references are listed in [9] and many more studies have been documented only as company reports, such as [10]. Some of the previous work is limited for one or more of the following reasons.

1) Important error sources, especially model errors are neglected.
2) Only linearized covariance results are presented.
3) A single sensor type is studied.
4) Orbit-dependent results apply to a narrow class of orbits, with low altitude orbits most common.

When taken collectively, previous studies provide a fairly complete answer to the problem of satellite navigation for near-earth orbits. At high altitudes, defined here as altitudes in the range of 5000 to about 60 000 nautical miles, considerably fewer results are available. These are contained principally in [8] and [10] and they also suffer from some of the limitations mentioned above.

At high altitudes the geometric scale, the dynamic rates of change, and the relative importance of several phenomenological problem variables are significantly different from those at low altitudes. It has never been demonstrated that low altitude results can be reliably extrapolated to high altitudes. This paper summarizes an extensive study of high altitude navigation systems. The purpose of this study is to determine what types of navigation sensors are feasible for use in high altitude missions which are planned or projected out to the year 1985. Realistic estimates of system performance, defined in terms of navigation accuracy and initial convergence time, are the principal components used in determining feasibility.

Of necessity, this study considers an extensive set of candidate navigation systems, a wide range of orbit geometry (altitude, eccentricity, inclination), realistic models for sensor errors and phenomenology effects, and several complementary methods of obtaining measures of performance. From the wide spectrum of simulation results, only representative examples and summary results are presented because of space limitations. A more extensive presentation of detailed results is contained in [11].

## II. Study Methodology

The method of evaluating system performance is direct Monte Carlo simulation. The philosophy which underlies all simulations in this study is illustrated in Fig. 1, which is adapted from [3]. The diagram divides into two parts. One part, sometimes called the message and observation

Manuscript received August 16, 1974; revised July 9, 1975. Paper recommended by G. Stein, Past Chairman of the IEEE S-CS Applications, Systems Evaluation, Components Committee.

J. L. LeMay, C. E. Seal, and H. T. Hendrickson are with the Aerospace Corporation, El Segundo, Calif. 90045.
W. L. Brogan is with the Department of Electrical Engineering, University of Nebraska, Lincoln, Nebr. 68508.